

MHD modeling of ELM physics and RMPs in view of DTT

M. Calcagno^{1,2}, A. Cathey³, D. Bonfiglio^{1,4}, L. Pigatto¹, S. Cappello^{1,4}, M. Hoelzl^{3,5},

J. Puchmayr³, M. Veranda^{1,4}, and G. Vlad⁶

¹*Consorzio RFX (CNR, ENEA, INFN, Università di Padova, Acciaierie Venete SpA), Italy*

²*CRF - University of Padova, Italy*

³*Max Planck Institute for Plasma Physics, Garching b. M., Germany*

⁴*Istituto per la Scienza e la Tecnologia dei Plasmi, CNR, Padova, Italy*

⁵*Department of Physics and Astronomy, Chalmers University of Technology, Göteborg, Sweden*

⁶*Consorzio CREATE, Napoli, Italy*

Introduction.

The edge region of tokamaks can be subject to plasma instabilities, called Edge Localized Modes (ELM), that can release large heat loads on the divertor. ELMs are caused by the presence of steep pressure gradients and associated large current density in the so-called pedestal region, typical of H-mode confinement. It was demonstrated [1] [2] that the application of Resonant Magnetic Perturbations (RMP) can allow the mitigation or suppression of ELMs

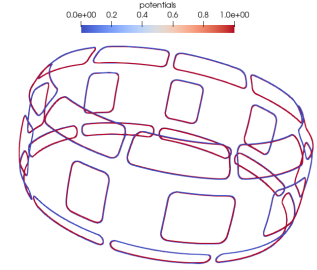


Figure 1: RMP coils in DTT implemented with STARWALL.

by reducing the pedestal gradients through the formation of magnetic islands and stochasticity. This work investigates peeling-ballooning stability and RMP optimization for ELM control in the Divertor Tokamak Test facility (DTT), an experiment under construction in Frascati (Italy) with the goal of exploring different divertor configurations (here the single-null is considered), and equipped with a set of 3 arrays of 9 RMP coils (NAS coils) (see fig.1). The following results refer to the full power scenario E with plasma current $I_p = 5.5MA$ and vacuum toroidal magnetic field $B_{tor} = 5.8T$ [3]. A reduced power scenario A ($I_p = 2MA$, $B_{tor} = 3T$) has also been implemented. Both the 3D non-linear visco-resistive MHD code JOREK [4] and the linear resistive MHD code MARS-F are employed to characterize peeling-ballooning instabilities, likely associated with ELM onset, developing in the plasma. In JOREK, the 3D RMP coils are modeled and discretized via a coupling to the STARWALL code, while the influence of other conducting structures on the MHD modes is neglected. In order to achieve a satisfying plasma response to the RMP application, MARS-F is used for the RMP spectrum optimization, in terms of phasing between the three RMP coil arrays [5]. The optimized RMPs can then be included in JOREK to study their interaction with ELMs [1].

Simulation Setup and Results. The DTT scenarios have been processed with the equilibrium code CHEASE, in order to compute the $n=0$ equilibrium in terms of a 2D (R,Z) grid to be given as input to MARS-F for the plasma response studies. Figure 2 shows the safety factor q and pressure profiles. In order to simplify the JOEREK modeling, the core region of the q profiles was modified to ensure that $q > 1$ throughout the plasma to avoid the presence of inter-

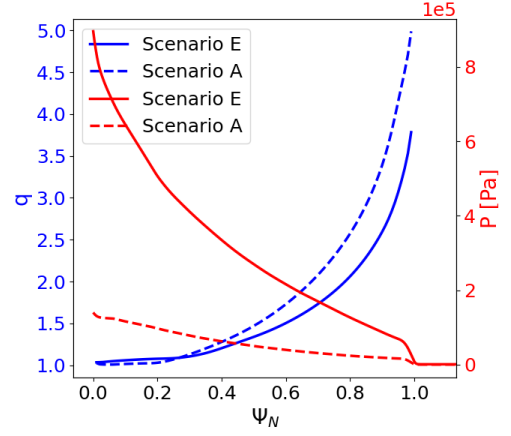


Figure 2: Pressure and safety factor profiles of JOEREK inputs for DTT scenarios A and E.

nal kink (sawtooth) instabilities. The electron density and temperature profiles are provided by the integrated modeling code-suite JETTO-JINTRAC. In JOEREK, the equilibrium state containing the $n=0$ plasma flow must be computed before adding the non-axisymmetric toroidal harmonics, and the plasma profiles are kept steady through the adequate balance between diffusion and source terms. The linear stability analysis with JOEREK was initially carried out excluding terms related to plasma flow, such as diamagnetic effects. These shall be included in addition to the ExB drift because of the crucial role of the electron perpendicular velocity played in RMP penetration [6], which occurs dominantly at the edge because of the increase in resistivity η , having assumed a Spitzer profile. The input pedestal profiles in DTT scenarios were optimized with the EPED stability workflow, which identifies the pedestal at the ideal MHD stability boundary. Consistently, the equilibrium has been found to be stable in JOEREK at realistic Spitzer resistivity $\eta_{SP} = 5 \cdot 10^{-9} \Omega m$, testing a range of toroidal mode numbers n ranging from 1 to 21. Therefore, in the following, some preliminary results are presented with increased $\eta \sim 10 \cdot \eta_{SP}$, which allowed to de-stabilize the modes of interest. In MARS-F, the MHD equations are solved only up to the last closed flux surface ($\psi_N \sim 0.99$), and the no-wall approximation is assumed, consistently with JOEREK-STARWALL simulations. The values of the RMP coil currents depend on the coil geometry and on the selected n . Also in the MARS-F simulations, the JETTO-JINTRAC kinetic profiles were implemented, namely temperature, density, toroidal rotation profile, and η follows a Spitzer profile. In addition, a viscous source mimics the parallel sound wave (Landau) damping effect.

Toroidal mode number scans of the growth rate of the unstable modes performed with JOEREK with increased η revealed the presence of structures strictly localized at the edge and in the so-called "bad-curvature" region, i.e. where the sign of the product $\vec{\nabla} P \cdot \vec{k}$ is positive, allowing for

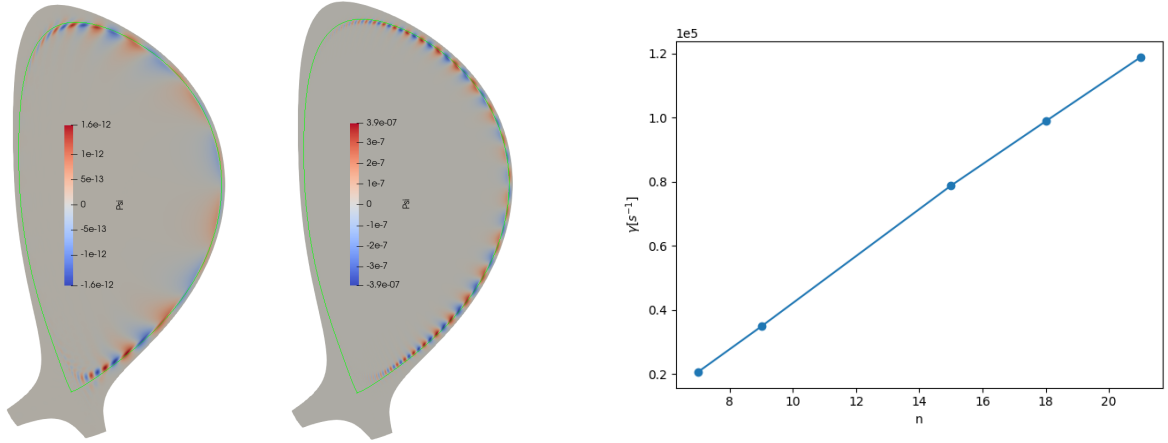


Figure 3: In the case at higher η without diamagnetic flows, from left to right: The poloidal structure of the $n=7$ modes (poloidal magnetic flux), of the $n=21$ modes, and variation of the growth rate of the PB instabilities with n . the destabilization of the modes. Fig.3 shows an example with $\eta \sim 8 \cdot 10^{-8} \Omega m$ and exhibits the peeling-ballooning (PB) nature of these modes, which are strong candidates for ELMs precursors, with the typical double dependence on the pressure gradient and current density. Fig.3 also shows how the growth rate of this kind of instabilities increases in magnitude as n increases. The grid resolution required to better resolve such radially thin edge structures has been investigated to ensure convergence of the growth rate. In particular, the growth rate was found to converge at sufficiently high poloidal resolution, and the shape of the respective eigenfunctions at different resolutions is the same, suggesting that the underlying physics is correctly captured. An analogous linear study has been carried out with MARS-F, which also revealed the presence of PB structures. MARS-F has been used to calculate the plasma response to external perturbations with $n=1,2,3$.

In the $n=2$ perturbation case, the vacuum spectrum shows $m=5,6,7,8$ resonant peeling components screened by the plasma, while the non-resonant components both in the $m < 0$ and $m > 0$ parts of the spectrum are amplified. The resistive penetration effect is partially hindered by the low value of η , close

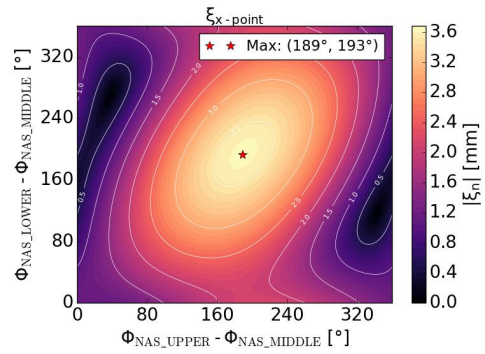


Figure 4: Displacement ξ induced by a $n=2$ perturbation produced by the three RMP coil arrays in the x-point region.

to the ideal limit. As mentioned previously, in DTT there are 3 arrays of RMP coils, for the optimization of the relative phasing, the middle array was considered to be at fixed phase Φ , while the upper and lower ones change with respect to it. The result is shown in terms of normal displacement of the plasma surface ξ in fig. 4, computed and averaged in a region selected as close as possible to the location of the X-point (absent in MARS-F). An induced displacement of 3.6 mm can be achieved when setting the total current of

the single coil (here, given by the sum of all turns) to the maximum allowed in DTT of 40 kA and with the optimal phasing of $\sim 190^\circ$ of both the upper and lower coil arrays with respect to the middle one. It is worth noting that here the JETTO-JINTRAC rotation profile with rotational frequency $\Omega_{axis} = 0.01\Omega_{edge}$ is likely to play a role, in addition to the low resistivity, in hindering RMP penetration. An RFX-mod2 [7] tokamak test case has also been implemented in JOREK in view of a benchmark with MARS-F in a simpler geometry. Similar plasma response and tearing mode linear stability studies will be performed.

Conclusions. A linear stability study of edge instabilities in DTT plasmas was performed with JOREK, confirming physical insights such as the peeling-ballooning nature of the plasma instabilities of interest, their spatial structure and the increase of the growth rates both with resistivity and toroidal mode number. MARS-F was employed to optimize the RMP coils phasing and currents to be implemented in JOREK-STARWALL. In terms of future work, a scan in rotational velocity is planned in order to quantify its effect on RMP screening, and the same rotational profiles are planned to be applied in JOREK simulations with RMPs. With JOREK, the aim is to study the isolated effect of RMPs on a stable plasma at physical resistivity with the DTT profiles in fig.2 without modes, and then on a de-stabilized scenario with higher pedestal pressure (P_{ped}) and gradient steepness to self-consistently model the interaction between penetrating RMPs and peeling-ballooning modes. In the reduced MHD model of JOREK [4], this is attained by adding external particle and heat sources. For this purpose, this study shall include diamagnetic flow effects, and the effect of the bootstrap current linked to the increased P_{ped} .

Acknowledgments. This work has been funded by the European Union - NextGenerationEU (Mission 4, Component 2), CUP C96E24000070004. This work has been carried out within the framework of the EUROfusion Consortium, funded by the European Union via the Euratom Research and Training Programme (Grant Agreement No 101052200). Views and opinions expressed are, however, those of the authors only and do not necessarily reflect those of the European Union or the European Commission. Neither the European Union nor the European Commission can be held responsible for them. The PhD Course is jointly delivered by University of Padova and University of Napoli Federico II. The research has been conducted at Consorzio RFX, ENEA third party in the EUROfusion Consortium.

References

- [1] M. Becoulet et al. In: *Nuclear Fusion* 62.6 (2022), p. 066022.
- [2] M. Willensdorfer et al. In: *Nature Physics* 20.12 (2024), pp. 1980–1988.
- [3] I. Casiraghi et al. In: *Plasma Physics and Controlled Fusion* 65.3 (2023), p. 035017.
- [4] M. Hoelzl et al. In: *Nuclear Fusion* 61.6 (2021), p. 065001.
- [5] L. Pigatto et al. In: *Nuclear Fusion* 64.1 (2023), p. 016023.
- [6] F Orain et al. In: *Physics of Plasmas* 20.10 (2013).
- [7] D. Terranova et al. In: *Nuclear Fusion* 64.7 (2024), p. 076003.